

# The Preparation, Characterization, and Influence of Multiple Electroless Nickel-Phosphorus (Ni-P) Composite Coatings on Poplar Veneer

Yanfei Pan, Xin Wang, and Jintian Huang\*

Nickel-Phosphorus (Ni-P) composite coatings were prepared on a poplar veneer surface *via* a simple electroless nickel (Ni) approach. The substrate deformation, flatness, crystalline structure, and wear resistance of the Ni-P composite coatings were investigated. The deformation degree of the substrate decreased as the number of deposition steps was increased. The flatness and wear resistance of the composite coatings were enhanced with the increase in the number of depositions. The full width, at half of the maximum values of Ni X-ray diffraction (XRD), of peaks in the composite coatings were broadened and strengthened with an increment of the number of depositions in the coatings. The XRD patterns revealed that the Ni that had been deposited on poplar veneer had a crystallite size structure between 42 and 88 Å. The composite structure was characterized with scanning electron microscopy (SEM) images. The uniformity of the particles in the composite coatings could be improved with the increase in the number of depositions. The wear resistance of ideal coatings with a homogeneous thickness was measured via the rolling wear testing machine (RWTM), and the wear resistance of the coatings was increased by 200% compared with that of coatings obtained *via* a single deposition.

*Keywords:* Poplar veneer surface; Electroless Ni-P; Deposition steps; Wear resistance

*Contact information:* College of Material Science and Art Design, Inner Mongolia Agricultural University, Hohhot 010018, China; \*Corresponding author: jintian\_h@163.com

## INTRODUCTION

Wood deformation is a common phenomenon that arises from moisture loss and poor wear resistance. Such deformation can seriously restrict the application of metallization wood, even when the evenness of metallization coatings is outstanding. More than half of the sum of energy consumption may be the result of reactive power loss in all forms (Ge *et al.* 1991). In particular, the proportion of mechanical parts that fail due to various forms of wear has been found to be as high as 80% (Ge *et al.* 1991). The mechanism of wear can be divided into abrasive wear, adhesive wear, fatigue wear, corrosion wear, erosion wear, and fretting wear. The main wear types have been found to be abrasive wear and adhesive wear (Liu *et al.* 1993). A wood surface was treated *via* an electroless approach to form a metal coating on the wood surface, a process that is defined as wood metallization (Xiao 2004). The wear, anti-corrosion, and decoration of metallized wood were enhanced by new higher performance on wood. Wood metallization has had advantages in the preparation of various kinds of handicrafts and signage (Pi and Wang 2006). Favorable aspects of using wood in such cases include the fact that a wood-based composite material can keep its natural characteristics, insulation performance, and high strength (Nagasawa

*et al.* 1999; Zhou *et al.* 2000). During the past five decades, electroless plating has gained popularity due to prepared coatings that possess excellent corrosion, wear, and abrasion resistance. Among the variety of plated metals by this method, electroless nickel has proved its supremacy because of the ability to prepare coatings with excellent corrosion and wear resistance (Gavrilov 1979; Riedel 1991). A large number of research projects on modified wood have also been performed (Bakraji *et al.* 2001, 2002, 2003; Ebner and Petutschnigg 2007). Recently, progress in electroless nickel plating and its alloys have been reported. These have been applied on wood surfaces to improve their properties, such as electrical conductivity and electromagnetic shielding effectiveness (Nagasawa *et al.* 1999; Li *et al.* 2010; Wang *et al.* 2011). Huang and Li (2003) and Jing *et al.* (2005) conducted previous preliminary studies on wear resistance of Ni-P composite coatings. Pan *et al.* (2014) conducted further studies on the wear resistance of nano-SiC reinforced Ni-P composite coatings. However, there have been no reports concerning electroless nickel coating process on poplar veneer samples, to improve the wear resistance and decrease the deformation degree of wood based composite materials. The method of multiple electroless Ni is simple and is an easy way to improve the performance of coatings. This article reports a simple electroless Ni coating process on four pretreated wood samples to improve the wear resistance of the coatings. The relationship of the mass loss (ML) of nickel as a function of the number of deposition steps that were carried out on the four samples was also examined, and the nickel coatings after different times of deposition were characterized using SEM, RWTM, and XRD.

## EXPERIMENTAL

### Reagents and Materials

The reagents nickel sulfate (as a source metal), sodium hypophosphite (as a reducing agent), sodium citrate (as a complexing agent), thiourea (as a stabilizer), and ammonia (for pH adjustment) were analytically pure. The materials used were poplar veneer (as a substrate material) and sand paper (#600).

**Table 1.** Composition of Electroless Plating Bath

Bath component	Content
Nickel sulfate (analytically pure)	0.1267 mol•L <sup>-1</sup>
Sodium hypophosphite (analytically pure)	0.3267 mol•L <sup>-1</sup>
Sodium citrate (analytically pure)	0.1033 mol•L <sup>-1</sup>
Thiourea (analytically pure)	10 mg•L <sup>-1</sup>
Ammonia (analytically pure)	30 mL•L <sup>-1</sup>

### Preparation of Metallization Wood

Layers of poplar veneer were cut into sizes of 4.5 cm (radius) × 0.15 cm (thickness) and polished. The pieces of poplar veneer were then rinsed in deionized water at 100 °C for 15 min with constant agitation to remove any dust, and subsequently dried in a DH-101-2-S-type electric drum wind drying oven, at 100 °C for 15 h to determine the dry weight before the pretreatment was applied. Then, the poplar veneer was activated in

solution A (NiSO<sub>4</sub> and HCl, which were analytically pure, Tianjin, China), and the samples were taken out until there was no excess liquid dripping from the wood. The samples were then activated in solution B (NaBH<sub>4</sub> and NaOH, which were also analytically pure, Tianjin, China). The poplar veneer samples were taken out until there was no excess liquid dripping. Electroless nickel coatings were performed at 60 °C for 30 min, and the pH value of the solution was 9. During electroless nickel coatings, the bath was agitated manually to both homogenize the bath solution, and eliminate the gas bubbles from the poplar veneer surface during plating. Finally, the samples were washed with deionized water for 10 sec, and then dried in an oven at 100 °C for 10 h to obtain the composite material via one deposition. The above-mentioned steps were repeated four times. After each electroless nickel coating, the samples were rinsed with deionized water for 10 sec and then dried at 100 °C for 10 h. Finally, the solids were dried for 30 min in a vacuum oven (DH-101-2-S-type) in order to measure the other properties.

**Table 2.** Composition of Activation Solution

Component	Content
NiSO <sub>4</sub> (analytically pure)	15g•L <sup>-1</sup>
HCl (analytically pure)	12mL•L <sup>-1</sup>
NaBH <sub>4</sub> (analytically pure)	15 g•L <sup>-1</sup>
NaOH (analytically pure)	12 g•L <sup>-1</sup>

## Surface Characterization

### *Digital camera*

A Nikon Power Shot G1 X Mark II camera was used.

### *Scanning electron microscopy*

The coating surface morphology and cross section were obtained using S-3400N, SU8020 and S4800 SEM system.

### *X-Ray Diffraction (XRD) spectra*

XRD patterns were obtained with a D8 Advance diffractometer (Bruker) using monochromatic CuKα1 radiation ( $\lambda = 1.5406 \text{ \AA}$ ). The patterns were scanned over the angular range of 20 to 85° (2 $\theta$ ), with a step length of the (PSD) of 0.08° (2 $\theta$ ), over a 20 sec time frame.

### *Wear resistance test*

The wear resistance was tested on the plated poplar veneer surface via an MMG-5 rolling wear testing machine, accounting for a time of 20 sec per weighing each poplar veneer mass. The wear resistance rate (WRR) was calculated based on Eq.1,

$$v = \frac{m_1 - m_0}{s t} \quad (1)$$

where,  $v$  equals the wear resistance rate (g/cm<sup>2</sup>•s),  $m_1$  stands for the mass of the poplar veneer before the wear test (g),  $m_0$  is the mass of the poplar veneer after the wear test (g),  $s$  is the surface area of wood (cm<sup>2</sup>), and lastly  $t$  is the time of the abrasion test (s).

## RESULTS AND DISCUSSION

### Metallization Poplar Veneer Surface Morphology

Figure 1(a) shows that the coating imparted a black-grey coloration, and the bending deformation was obvious. The coating color was light grey, and the deformation degree decreased gradually with increasing treatment with the electroless coating. Figure 1(c) in comparison with Figs. 1(a) and 1(b), shows that the coating color was bright grey, which is a characteristic color of the Ni metal. Meanwhile, evidence of deformation had disappeared, and the coating was a metallic bright color, as shown in Fig. 1(d).

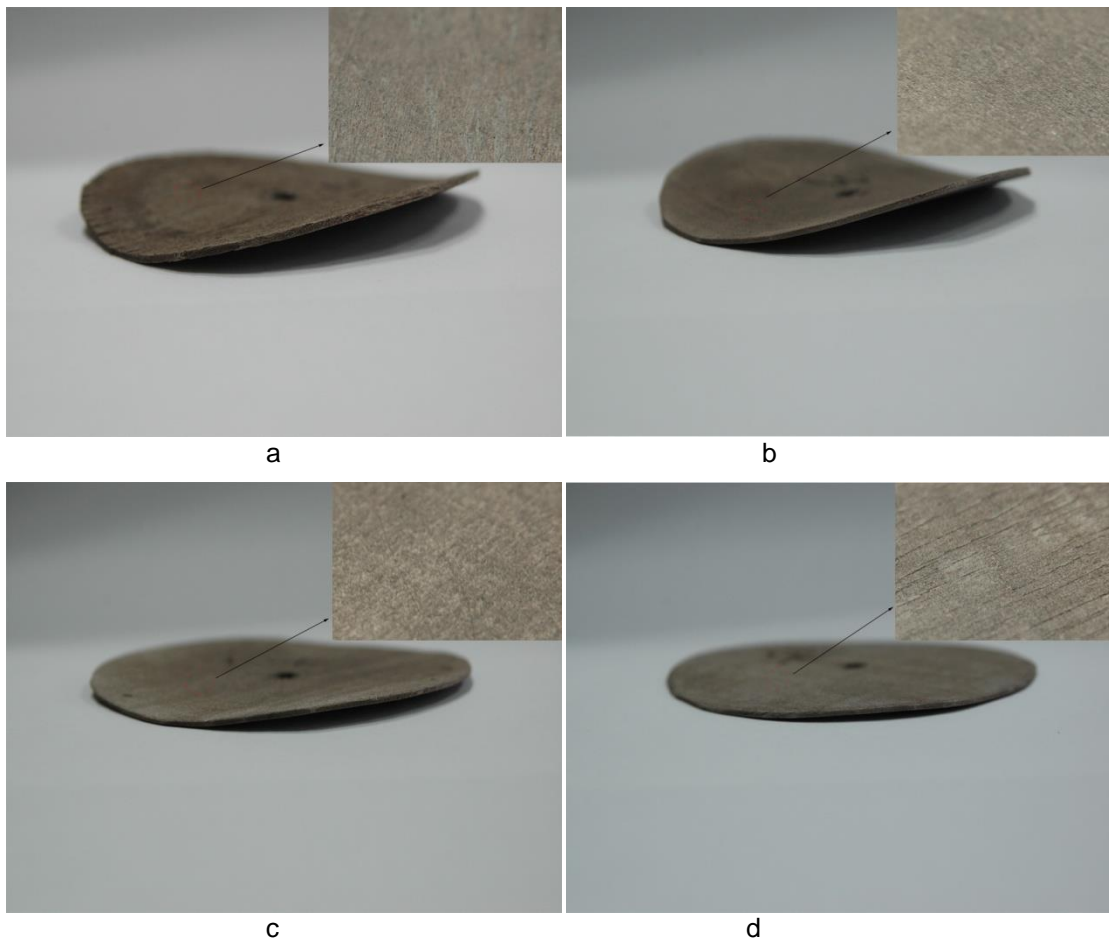


**Fig. 1.** Metallization poplar veneer morphology (a) one deposition, (b) two depositions, (c) three depositions, (d) four depositions

The ideal composite coatings without obvious bending deformation could be obtained when four depositions had been applied. The strength and flatness of the composite was improved with the increase in the number of depositions. The catalytic activity of the metal particles plays an important role in electroless plating, namely in an autocatalytic electroless process. Based on previous research it was expected that metal ion deposition would be dependent on the catalytic activity of substrate. It has been found that when a substrate is completely covered by metal, the autocatalytic reaction immediately stops unless the deposited coatings have catalytic activity (Nagasawa *et al.* 1999).

### Scanning Electron Microscopy (SEM) Morphology

Figure 2(a) shows that the poplar veneer surface was covered by metal Ni and the pores were directly filled by the metal Ni. There were some ravines formed on poplar veneer surface, and some of the Ni particles whose sizes were no larger than 10  $\mu\text{m}$  were surrounded by a black flaky-shaped substance. The flakes were agglomerated together, as shown in Fig. 2(a) and 2(b).

In Fig. 2(a) and (b), it can be observed that some isolated voids on poplar veneer surface were as large as 20  $\mu\text{m}$ . The number of the ravines that formed had decreased, and these large voids in Figs. 2(a) and (b) decreased distinctly, as can be seen in Fig. 2(c), while increasing the quantity of Ni deposited after three electroless nickel coatings. Moreover, the black flaky-shaped substance around the Ni had disappeared, and the distribution of the metal particles in the coatings was band-shaped.

Figure 2(d) shows that the distribution of the metal particles was flaky-shaped rather than band-shaped, indicating that the growth system of the Ni had changed. The metal Ni coated extent was in good condition, the structure was compact, and there were few small particles on the surface. The nickel clusters were nucleated uniformly on the surface, and these agglomerations are clearly not observed in Figs. 2(c) and (d). The energy diffraction spectrum demonstrated that the bright metal was mainly Ni particles and the black flaky-shaped substance was P and NiO (Table 3) in good agreement with Fig. 2(e), which further proved that a uniform and compact coating via electroless Ni can be obtained on a poplar veneer surface via four deposition steps.

**Table 3.** Energy-dispersive X-ray spectroscopy (EDS) of Coatings

Type of deposited coating	Composition (wt %)		
	Ni	O	P
One deposition	53.93	23.36	5.20
Two depositions	74.82	9.47	1.25
Three depositions	76.30	5.43	1.19
Four depositions	91.08	3.14	2.17

### Cross-Section Morphology

In Fig. 3, it can be observed that metal Ni had penetrated the cross-sections of coatings which varied in thickness between 162 and 290  $\mu\text{m}$  (Figs. 3(a), (b), (c), and (d)). Figure 3(e) shows that the pores of poplar veneer surface were covered by metal Ni, and the coatings were as thick as 290  $\mu\text{m}$  (Fig. 3(d)). The Ni had infiltrated the porous texture of wood, as shown in Fig. 3(c), and the ideal coating with the uniform thickness could be obtained when four depositions had been completed, as can be seen in Fig. 3(d). The pores on the poplar veneer surface were full of metal Ni, indicating that uniform and compact coatings can be obtained.

Figures 3(a), (b), (c), and d clearly show that the composite coatings increase in the number of deposition steps. A cross-sectional image of Fig. 3(e) showed that Ni had infiltrated the porous texture of poplar veneer and exhibited excellent adherence between the poplar veneer and Ni coating. However, similar results could not be obtained from the other samples in Figs 3a, b and c because less than four depositions were completed for that sample. The pores were filled, and the poplar veneer surface was wholly and compactly covered by Ni metal, as shown in Fig. 3(f). An ideal interface combination between the poplar veneer and Ni layer could be obtained with four depositions.

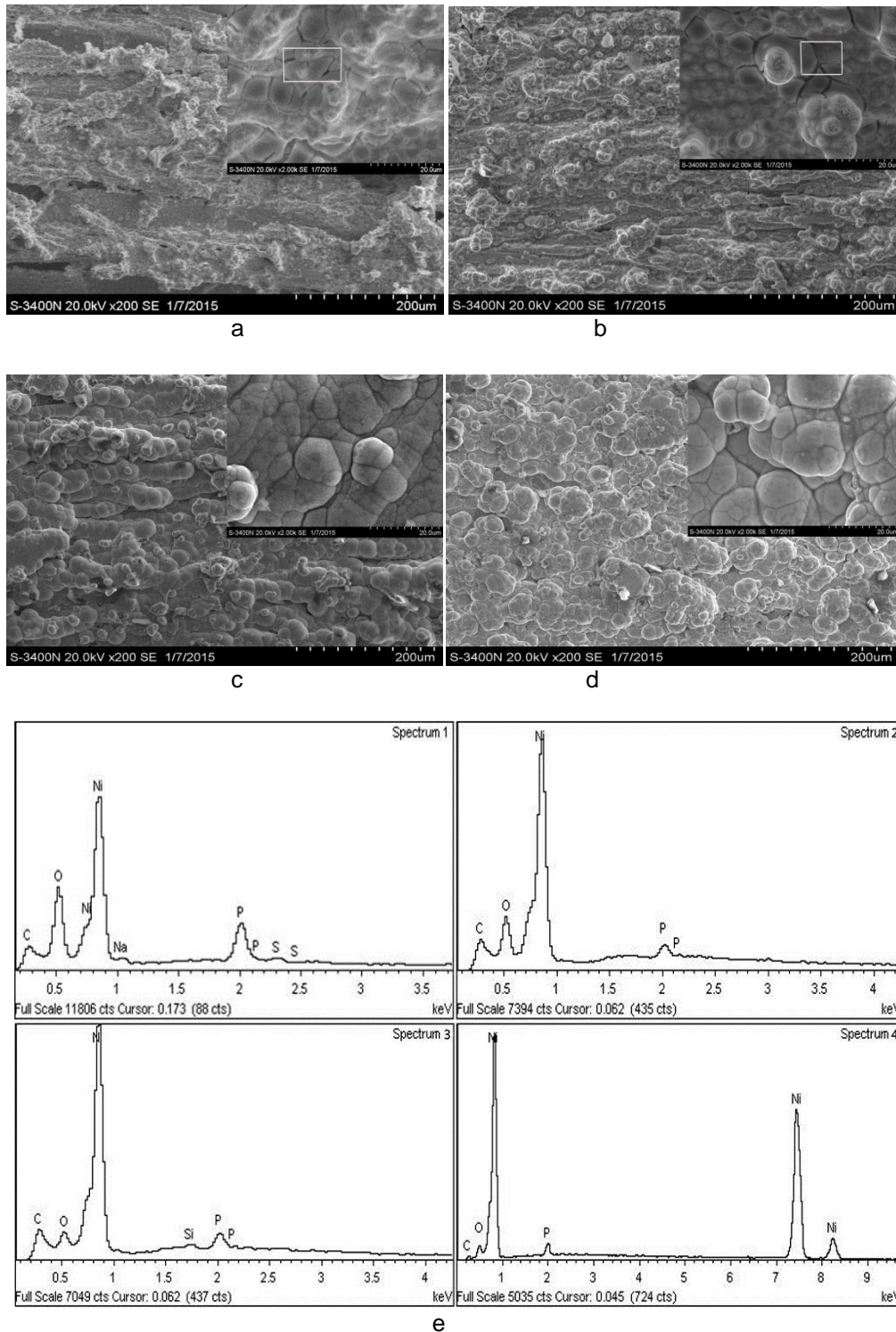


**Fig. 2.** Surface morphology of metallization poplar veneer *via* different deposition run (a) one deposition (inset shows the amplification image), (b) two depositions (inset shows the amplification image), (c) three depositions (inset shows the amplification image), (d) four depositions (inset shows the amplification image), (e) energy spectrum diagram of poplar veneer surface *via* different deposition steps (1: one deposition, 2: two depositions, 3: three depositions, 4: four depositions)

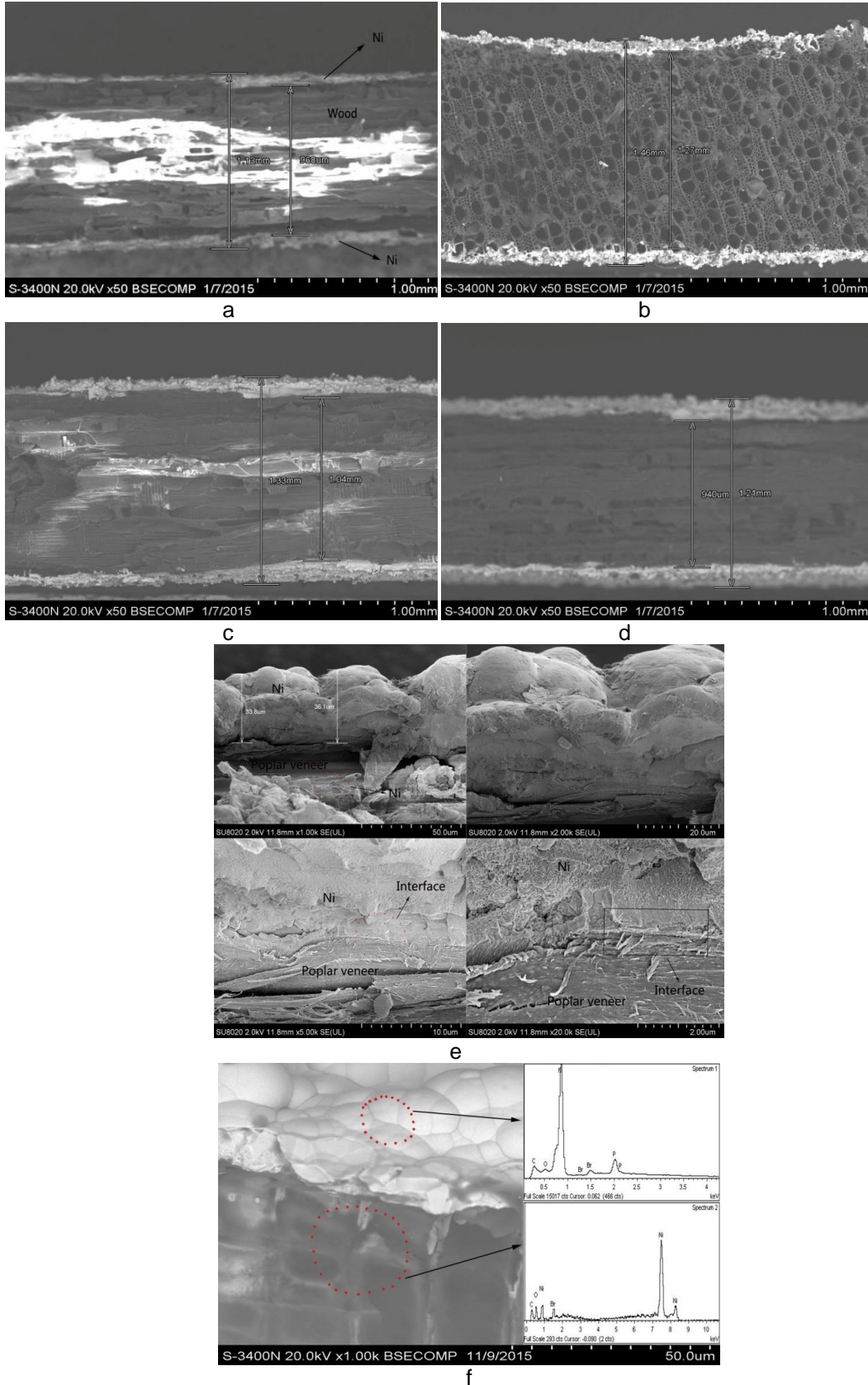


**Fig. 3.** Cross-section morphology: (a) 1 deposition, (b) 2 depositions, (c) 3 depositions, (d) 4 depositions, (e) interface of composite coatings with amplified images, (f) interfacial morphology

### X-Ray Diffraction (XRD) Analysis

Figure 4(a) shows the XRD pattern of the uncoated poplar veneer. A characteristic diffraction peak corresponding to poplar veneer peak at  $2\theta = 22^\circ$  appeared. It can be clearly observed from Fig. 4(b) that the crystalline structure significantly increased as the diffraction peaks of the Ni (111), Ni (200), and Ni (220) appeared. A new diffraction peak corresponding to the Ni peak appeared as shown in Fig. 4(b). Those diffraction peaks further illustrated the presence of Ni particles on the poplar veneer surface. Comparing Fig. 4(a) with Fig. 4(b), there is indication of the transformation of crystalline structure on the surface. Nonmetallic materials were transformed into metallic and magnetic composite materials via a simple electroless Ni-P approach.

The diffraction peaks in the range of 20 to  $85^\circ$  were identified and fitted using a pattern fitting module available with the software Jade.5.

In Fig. 4(b), it can be observed that the diffraction peaks at  $2\theta=44.5^\circ$ ,  $51.84^\circ$ , and  $76.37^\circ$  were broadened and strengthened because of Ni (111), Ni (200), and Ni (220) which showed the face-centered cubic phase of Ni (PDF: 65-2865), and indicated the crystalline nature of the film (Amer 2014). The full width, at half of the maximum values of the Ni XRD peaks at  $2\theta=44.5^\circ$ ,  $51.84^\circ$ , and  $76.37^\circ$ , in the composite coatings were broadened and strengthened, which demonstrated that the structure of the wood surface did not have an obvious change, and the grain size of the composite coatings can be refined as expressed in Table 3.

The diffraction peaks of the Ni (111), Ni (200), and Ni (220) increased with an increasing number of depositions, while diffraction peaks of poplar veneer gradually decreased in the number of deposition steps, which indicated that the poplar veneer surface had been completely covered by the metal composite coatings in view of the XRD analysis. The peak positioned at  $2\theta=65^\circ$  appeared after coating, and it disappeared with the increasing the number of depositions. It is possible reason that the NiO peak at  $2\theta=65^\circ$  was due to species already present in the electroless solution. The NiO was gradually coated by metal Ni with the increasing the number of depositions. The peak at  $2\theta=65^\circ$  disappeared as the compact and homogeneous coatings can be obtained.

The crystallite sizes of Ni ( $D \text{ \AA}$ ) were calculated from the integral breadth of the Ni (111) peak via Sherrer's Equation based on Eq. 2,

$$D = \frac{\kappa\lambda}{\beta \cos \theta} \quad (2)$$

where,  $\kappa$  is Sherrer's constant ( $\kappa=1$ ),  $\lambda=1.5406\text{\AA}$  is the X-ray wavelength,  $\beta$  is the integral breadth of a reflection (in radians) located at  $2\theta$ , and  $\theta$  is the angle of Bragg diffraction.

The experimental results showed that the Ni crystallites grew rapidly with the increasing in number of deposition steps as shown in Table 4.

**Table 4.** Integral Breadth Values and Calculated Values of the Crystallite Size of the (111) Nickel Peak as a Function of the Number of Depositions

Number of depositions	Integral Breadth $\beta$ (radians)	Calculated crystallite size (D) ( $\text{\AA}$ )
One deposition	2.032	42
Two depositions	1.244	69
Three depositions	1.082	80
Four depositions	0.982	88

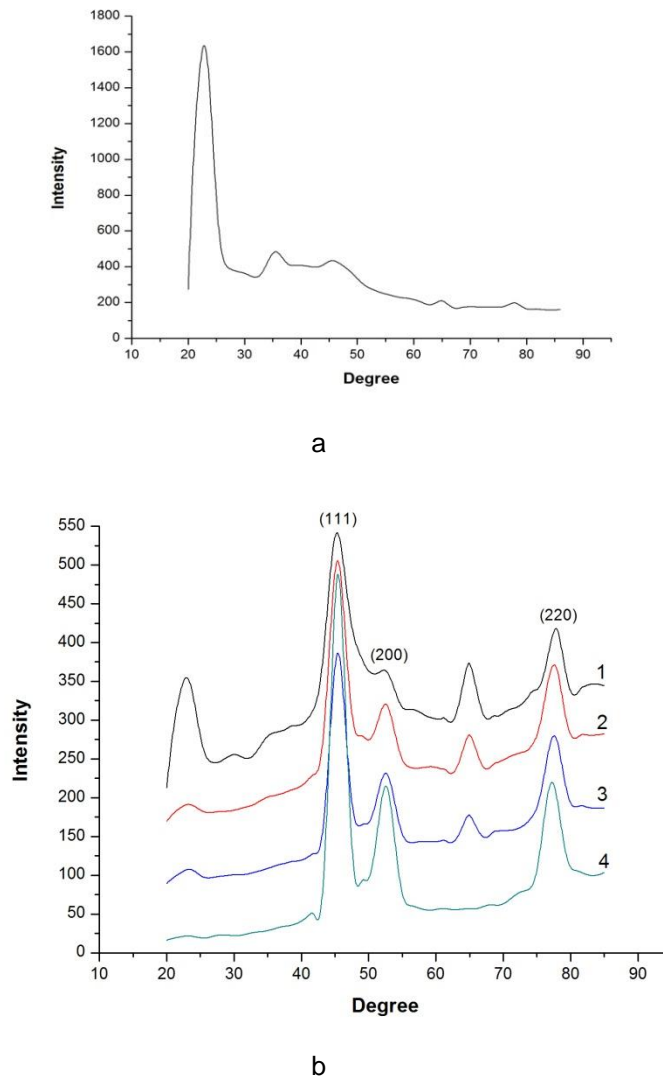


**Fig. 4.** XRD analysis (a) XRD pattern of uncoated poplar veneer, (b) coated poplar veneer: (1) one deposition, (2) two depositions, (3) three depositions, (4) four depositions

### Wear Resistance

Figure 5 shows the relationship between wear mass loss and the number of depositions. These curves show that the maximum amounts of wear were significantly different (Table 5). All of the coatings experienced a nearly similar amount of wear mass loss before 50 sec. However, the coatings exhibited a varying degree of wear mass loss after 50 sec, as shown in Fig. 5. With the increase in time, the mass of the poplar veneer with uniform coatings gradually decreased. The wear resistance rate of curve 1 varied much faster compared to that of curves 2, 3, and 4, as shown in Fig. 5 and Table 5. The wear resistance rate was calculated based on Eq.1. The mass of the poplar veneer with one deposition decreased constantly up to 700 sec, while the mass of the poplar veneer with four depositions did not change after 100 sec, indicating that the abrasive resistance had increased seven times. Table 5 shows that the poplar veneer mass decreased by more than two times (200%), comparing one deposition with four depositions, which powerfully illustrated that the coatings via four depositions can exhibit excellent wear resistance. The

possible reason was that the original defects of the crystal lattice vacancies were improved with the increase in the number of depositions, triggering the metallic atoms in the crystal structure to be distributed uniformly and the crystal lattice defects to become enhanced. To some extent, this improved the micromechanics of the coating performance (Vaezi *et al.* 2008). Moreover, with the increase in number of deposition steps, the P content gradually decreased. The decrease of P content can affect the flatness and porosity of coatings, and improve the crystallinity of the coatings (Pan *et al.* 2014). Besides, the coatings hardness decreased in augment of P content in the coatings because low phosphorus content hindered the deformation of Ni lattice and keep the hardness of coatings (Lin *et al.* 2013). The P content decreased with an increasing number of deposition steps, indicating that the deformation degree of Ni lattice was increased. Here, the wear resistance of composite coatings was improved resulted from the increase in hardness. The experimental results were in conformity with the SEM analysis.

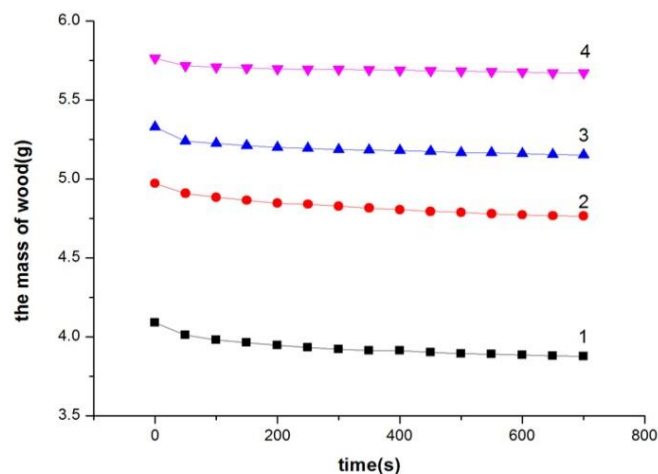


**Fig. 5.** The relationship between wear mass loss and the number of depositions: (1) one deposition, (2) two depositions, (3) three depositions, (4) four depositions

**Table 5.** The Relationship between Wear Mass Loss and the Number of Depositions

Number of depositions	Poplar veneer mass ( $m_1/g$ )	Poplar veneer mass ( $m_2/g$ )	Mass change ( $\sigma m/g$ )	WRR ( $g/cm^2 \cdot s$ )
One deposition	4.0903	3.8751	0.2152	$4.8 \times 10^{-6}$
Two depositions	4.9713	4.7648	0.2065	$4.6 \times 10^{-6}$
Three depositions	5.3286	5.1525	0.1761	$3.9 \times 10^{-6}$
Four depositions	5.7635	5.6700	0.0935	$2.1 \times 10^{-6}$

## CONCLUSIONS

1. Ni-P composite coatings were successfully prepared on a poplar veneer surface *via* a simple electroless Ni approach. The ideal composite coatings without obvious bending deformation could be obtained when four depositions were done.

2. The metal Ni coating extent was in good condition. The structure was compact, and the Ni was deposited at 290  $\mu\text{m}$  in depth when four deposition steps had been carried out. The Ni has infiltrated into the porous texture of the poplar veneer and exhibited excellent adherence between the wood and metal coatings.
3. The deposited Ni on poplar veneer surface had crystallite size in ranging from 4.2 to 8.8 nm with an increasing number of deposition steps according to XRD patterns. It is feasible to control the crystallite size and surface morphology of Ni particles *via* this method.
4. The wear resistance of the coatings *via* four depositions was increased by 200% compared with that of coatings prepared via one deposition. The decreasing in P content enhanced the wear resistance of composite coatings.

## ACKNOWLEDGMENTS

This work was supported by the National Natural Science Foundation of China under Grant No. 30960305, Inner Mongolia Autonomous Region applied technology research and development funds plan (20130317), and science research innovation projects of the Inner Mongolia Autonomous Region for graduate under Grant No.B20141012902Z.

## REFERENCES CITED

- Amer, J. (2014). "Influence of multiple electroless nickel coatings on beech wood: Preparation and characterization," *Composite Interfaces* 21(3), 191-201. DOI: 10.1080/15685543.2014.854615.
- Bakraji, E. H., and Salman, N. (2003). "Properties of wood-plastic composites: Effect of inorganic additives," *Radiation Physics and Chemistry* 66(1), 49-53. DOI:10.1016/S0969-806X(02)00262-1.
- Bakraji, E. H., Salman, N., and Al-kassiri, H. (2001). "Gamma-radiation-induced wood-plastic composites from Syrian tree species," *Radiation Physics and Chemistry* 61(2), 137-141. DOI: 10.1016/S0969-806X(00)00430-8.
- Bakraji, E. H., Salman, N., and Othman, I. (2002). "Radiation-induced polymerization of acrylamide within Okoume (*Aucoumea klaineana* Pierre)," *Radiation Physics and Chemistry* 64(4), 277-281. DOI:10.1016/S0969-806X(01)00579-5.
- Ebner, M., and Petutschnigg, A. J. (2007). "Potentials of thermally modified beech (*Fagus sylvatica*) wood for application in toy construction and design," *Materials Design* 28(6), 1753-1759. DOI: 10.1016/j.matdes.2006.05.015.
- Gavrilov, G. G. (1979). *Chemical (Electroless) Nickel-Plating*, Portcullis Press, Surrey, UK.
- Ge, Z. M., Hou, Y. J., and Wen, S. T. (1991). *Design of Wear-Resistance*, China Machine Press, Beijing, China, 6, 1-2 (in Chinese).
- Huang, L. G., and Li, S. Z. (2003). "Tribological behavior of electroless plating Ni-P deposits under dynamic loading," *China Surface Engineering* 15(1), 27-30. (in Chinese) DOI: 1007-9289(2003)01-0027-04.

- Jing, H., Lu, G. Z., Cai, G. Y., and Ma, Z. (2005). "Abrasivity study of different types of electroless nickel deposits," *Electroplating and Finishing* 24(2), 4-6. (in Chinese) DOI: 1004-227X (2005)01-0004-03.
- Li, J., Wang, L., and Liu, H. (2010). "A new process for preparing conducting wood veneer by electroless nickel plating," *Surface and Coatings Technology* 204(8), 1200-1205. DOI:10.1016/j.surfcoat.2009.10.032.
- Liu, J. J., Li, S. Z., and Zhou, P. A. (1993). *The Theories of Materials Wear and their Wear Resistance*, Tsinghua University Press, Beijing, China, 11, 92 (in Chinese).
- Lin, C., Zhao, L. C., Zhao, H. F., and Wu, H. F. (2013). "Effect of phosphorous content on microstructure and wear resistance of electroless Ni -P alloy coatings on titanium alloy," *Journal of Materials Protection* 46(1), 5-7. (in Chinese) DOI: 1001-1560 (2013) 01-0005-03.
- Nagasawa, C., Kumagai, Y., Urabe, K., and Shinagawa, S. (1999). "Electromagnetic shielding particleboard with nickel-plated wood particles," *Journal of Porous Materials* 6(3), 247-254. DOI: 10.1023/A: 1009692232398.
- Pan, Y. F., Huang, J. T., Guo, T. C., and Zhang, S. B. (2014). "Nano-SiC effect on wood electroless Ni-P composite coatings," *Proceedings of the Institution of Mechanical Engineers, Part N: Journal of Nanoengineering and Nanosystems*, Epub ahead of print, April 22, 2014. DOI: 10.1177/1740349914530683.
- Pi, J. H., and Wang, Z. Z. (2006). "The research status quo of wood-metal composite materials," *Journal of Nan Jing Institute of Technology* (Natural Science Ed.), 4(2), 17-21 (in Chinese) DOI: 1672-2558(2006) 02-0017-05.
- Riedel, W. (1991). *Electroless Plating*, ASM International, Ohio.
- Vaezi, M. R., Sadrnezhad, S. K., and Nikzad, L. (2008). "Electrodeposition of Ni-SiC nano-composite coatings and evaluation of wear and corrosion resistance and electroplating characteristics," *Colloids Surface A* 315, 176-182. DOI: 10.1016/j.colsurfa.2007.07.027.
- Wang, L., Li, J., and Liu, H. (2011). "A simple process for electroless plating nickel-phosphorus film on wood veneer," *Wood Science and Technology* 45(1), 161-167. (in Chinese) DOI: 10.1007/s00226-010-0303-0.
- Xiao, W. H. (2004). "The metallization methods on nonmetallic material surface," *Conservation and Utilization of Mineral Resources* 131(3), 28-31. (in Chinese) DOI: 1001-0076(2004) 03-0028-04.
- Zhou, Z., Cao, J. C., and Tang, P. Z. (2000). "Particleboard overlaid with aluminium foil," *China Wood Industry* (in Chinese), 14(1), 32-34. DOI: 1001-8654(2000) 01-0032-03.

Article submitted: September 17, 2015; Peer review completed: November 1, 2015;  
Revised version received: November 9, 2015; Accepted: November 10, 2015; Published:  
November 25, 2015.

DOI: 10.15376/biores.11.1.724-735